Journal of Quantitative Spectroscopy & Radiative Transfer ▮ (▮▮▮▮) ▮▮▮–▮▮▮

Contents lists available at ScienceDirect

Journal of Quantitative Spectroscopy & Radiative Transfer

journal homepage: www.elsevier.com/locate/jqsrt

Electromagnetic wave scattering from cuboid-like particles using *Sh*-matrices

Dmitry Petrov [a], Yuriy Shkuratov [a], Gorden Videen [b,*]

[a] *Astronomical Institute of Kharkov, V.N. Karazin National University, 35 Sumskaya St, Kharkov 61022, Ukraine*
[b] *Army Research Laboratory, AMSRD-ARL-CI-EM, 2800 Powder Mill Road, Adelphi, MD 20783, USA*

ARTICLE INFO

Article history:
Received 3 December 2009
Accepted 22 January 2010

Keywords:
Light scattering
T-matrix
Shape matrix
Cuboid

ABSTRACT

The *Sh*-matrix elements derived from the *T*-matrix technique allow one to separate the shape-dependent parameters from size- and refractive-index-dependent parameters. The separation also allows the corresponding surface integrals to be solved analytically for different particle shapes. In this manuscript we give analytical expressions for the *Sh*-matrix elements that contain the shape information for cuboid-like particles. We find very good agreement between the results obtained using the *Sh*-matrix method and those using the discrete-dipole approximation (DDA). The solution gives significant acceleration of calculations dependently on the size parameter of particles.

Published by Elsevier Ltd.

1. Introduction

Macroscopic objects and small particles whose shapes can be approximated by cuboids (parallelepipeds and prisms) are often encountered in nature. For instance, many different crystals can be described as cuboids [1]. Thus, the problem of electromagnetic wave scattering by such particles with size comparable to the wavelength is of interest in different fields of science (e.g., astrophysics, atmosphere and ocean optics, biophysics) and engineering (e.g., radar remote sensing, micro-technology).

The *T*-matrix method has been used to solve the light scattering from many non-spherical particles [2–6]. It is especially well suited for atmospheric aerosols as orientation averaging can be performed rapidly using analytical operations. This method can be applied to scattering by particles of arbitrary shapes; however, calculations for irregular particles are difficult and require significant computational expense to compute the surface integrals necessary to find the elements of the *T*-matrix [4]. Therefore, development of approaches allowing analytical computations of these integrals is beneficial.

Within the *T*-matrix technique, it has been shown that the shape-dependent factors can be separated from the size- and refractive-index-dependent factors and these are contained in the shape matrix, or *Sh*-matrix [4,6–13]. The elements of the *Sh*-matrix are expressed in terms of surface integrals. Once calculated, the *T*-matrix of particles that have other sizes and refractive indices can be found through analytical operations. In many cases the surface integrals describing the *Sh*-matrix elements themselves are sufficiently simplified as to be solvable analytically (e.g., for microlenses [6], Chebyshev particles [7], bi-spheres and capsules [8], merging spheres [9], finite cylinders [10], corrugated finite cylinders and capsules [11], cube-like particles [12], and all the mentioned particles with a concentric layered structure [13]). In this manuscript, we present an analytical solution for the *Sh*-matrix that can be used to find the electromagnetic wave scattering from cuboid-like particles with smooth edges and vertices. We present illustrations of the scattering from rectangular parallelepipeds.

* Corresponding author.
E-mail addresses: petrov@astron.kharkov.ua (D. Petrov), gvideen@arl.army.mil, gorden.videen@gmail.com (G. Videen).

0022-4073/$ - see front matter Published by Elsevier Ltd.
doi:10.1016/j.jqsrt.2010.01.024

Report Documentation Page

Form Approved
OMB No. 0704-0188

1. REPORT DATE	2. REPORT TYPE	3. DATES COVERED
DEC 2009		**00-00-2009 to 00-00-2009**

4. TITLE AND SUBTITLE	5a. CONTRACT NUMBER
Electromagnetic wave scattering from cuboid-like particles using Sh-matrices	5b. GRANT NUMBER
	5c. PROGRAM ELEMENT NUMBER
6. AUTHOR(S)	5d. PROJECT NUMBER
	5e. TASK NUMBER
	5f. WORK UNIT NUMBER
7. PERFORMING ORGANIZATION NAME(S) AND ADDRESS(ES) **Army Research Laboratory,AMSRD-ARL-CI-EM,2800 Powder Mill Road,Adelphi,MD,20783**	8. PERFORMING ORGANIZATION REPORT NUMBER
9. SPONSORING/MONITORING AGENCY NAME(S) AND ADDRESS(ES)	10. SPONSOR/MONITOR'S ACRONYM(S)
	11. SPONSOR/MONITOR'S REPORT NUMBER(S)

12. DISTRIBUTION/AVAILABILITY STATEMENT
Approved for public release; distribution unlimited

13. SUPPLEMENTARY NOTES

14. ABSTRACT
see report

15. SUBJECT TERMS

16. SECURITY CLASSIFICATION OF:			17. LIMITATION OF ABSTRACT	18. NUMBER OF PAGES	19a. NAME OF RESPONSIBLE PERSON
a. REPORT **unclassified**	b. ABSTRACT **unclassified**	c. THIS PAGE **unclassified**	**Same as Report (SAR)**	**8**	

2. *Sh*-matrices for right-cuboid-like particles

We consider a family of particles whose shapes transition from ellipsoids to cuboids expressed as follows:

$$R_0(n_0,\theta,\phi)=\left[(\sin\theta)^{n_0}\left(\left(\frac{\sin\phi}{b}\right)^{n_0}+\left(\frac{\cos\phi}{a}\right)^{n_0}\right)+\left(\frac{\cos\theta}{c}\right)^{n_0}\right]^{-1/n_0} \quad (1)$$

where θ and ϕ are the polar and azimuth angles, respectively. The parameters a, b, and c correspond to the half-lengths of the particle in the x, y, and z directions. When $a=b=c$ the particle has three-fold symmetry [12]. The parameter n_0 characterizes the similarity of the particle to a right parallelepiped (n_0 should be even). At $n_0=2$ the particle is an ellipsoid. As n_0 increases, the particle becomes less like an ellipsoid and more like a parallelepiped. Selected particle shapes are shown in Fig. 1. In the limiting case the equation for a parallelepiped is as follows:

$$R_0(\theta,\phi)=\lim_{n_0\to\infty}\left[(\sin\theta)^{n_0}\left(\left(\frac{\sin\phi}{b}\right)^{n_0}+\left(\frac{\cos\phi}{a}\right)^{n_0}\right)+\left(\frac{\cos\theta}{c}\right)^{n_0}\right]^{-1/n_0} \quad (2)$$

The *Sh*-matrix elements of particles whose shape is described by Eq. (1) can be expressed analytically. The derivation is extremely long and tedious, so we provide only the final equations describing the *Sh*-elements for cuboid-like particles in Appendix A. In the following sections we present results of calculations from sample particles, including comparisons with DDA simulations.

3. Calculations, results and discussion

In our calculations all particles are characterized with the refractive index m_0 and size parameter $X=2\pi r/\lambda$, where r is the radius of the circumscribing sphere, and λ is the wavelength. Fig. 2 shows maps of the light-scattering intensity distributions in the forward (a) and backward (b) hemispheres from cuboid-like particles ($m_0=1.33$ and size parameters $X_a=12$, $X_b=18$, and $X_c=24$). The distribution of the degree of linear polarization is presented in Fig. 2c (forward hemisphere) and Fig. 2d (backward hemisphere). The rows in these figures correspond to particle shapes changing from ellipsoid ($n_0=2$) at the top to more cuboid-like particles ($n_0=10$) at the bottom. The maps clearly demonstrate the transition from ellipsoid to cuboid. As the particle becomes more like a cuboid, the ellipsoidally shaped scattering fringes in the forward direction become more jagged and bright bands appear in the patterns in planes perpendicular to the surface facets. Differences are enhanced in the backscattering hemispheres. The columns correspond to the fixed orientation of particles at different angles φ of electromagnetic wave incidence. At $\varphi=0^\circ$ the incident wave propagates parallel to the normal of the largest cuboid face. At $\varphi=45^\circ$ the incident wave propagates at an angle 45° to this normal, and at $\varphi=90^\circ$, the incident wave propagates parallel to the normal to the smallest cuboid face. In the forward-scattering direction we can see that the fringe spacing is inversely proportional to the size parameter of the particle cross-section, with larger fringe spacing occurring in the plane corresponding to the smaller particle dimension.

Fig. 3 shows the normalized intensity and degree of linear polarization phase functions of cuboid-like particles averaged over orientation. Curves are shown for particles corresponding $n_0=2$ (solid lines), $n_0=4$ (dot lines), $n_0=6$ (dash-dot lines) and $n_0=10$ (lines with points), whose size parameters are $X_a=12$, $X_b=18$, $X_c=24$ and refractive index is $m_0=1.33$. As can be seen, the parameter n_0 noticeably

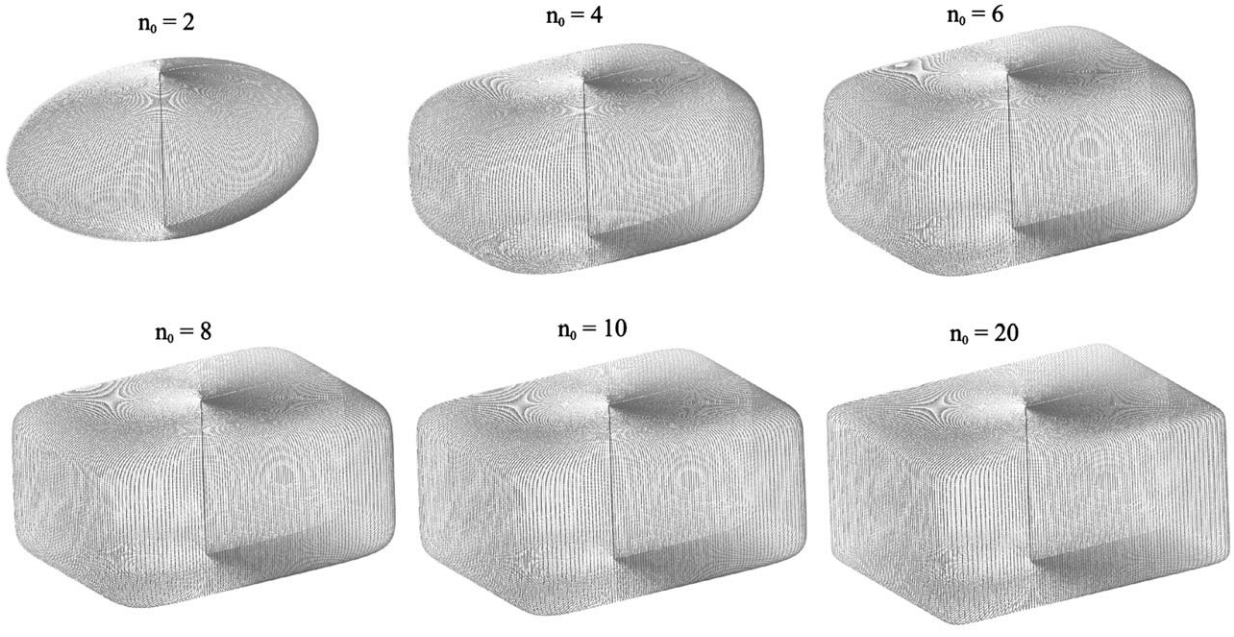

Fig. 1. Examples of cuboid-like particles at $a=1$, $b=0.75$, $c=0.5$, having different n_0.

Please cite this article as: Petrov D, et al. Electromagnetic wave scattering from cuboid-like particles using *Sh*-matrices. JQSRT (2010), doi:10.1016/j.jqsrt.2010.01.024

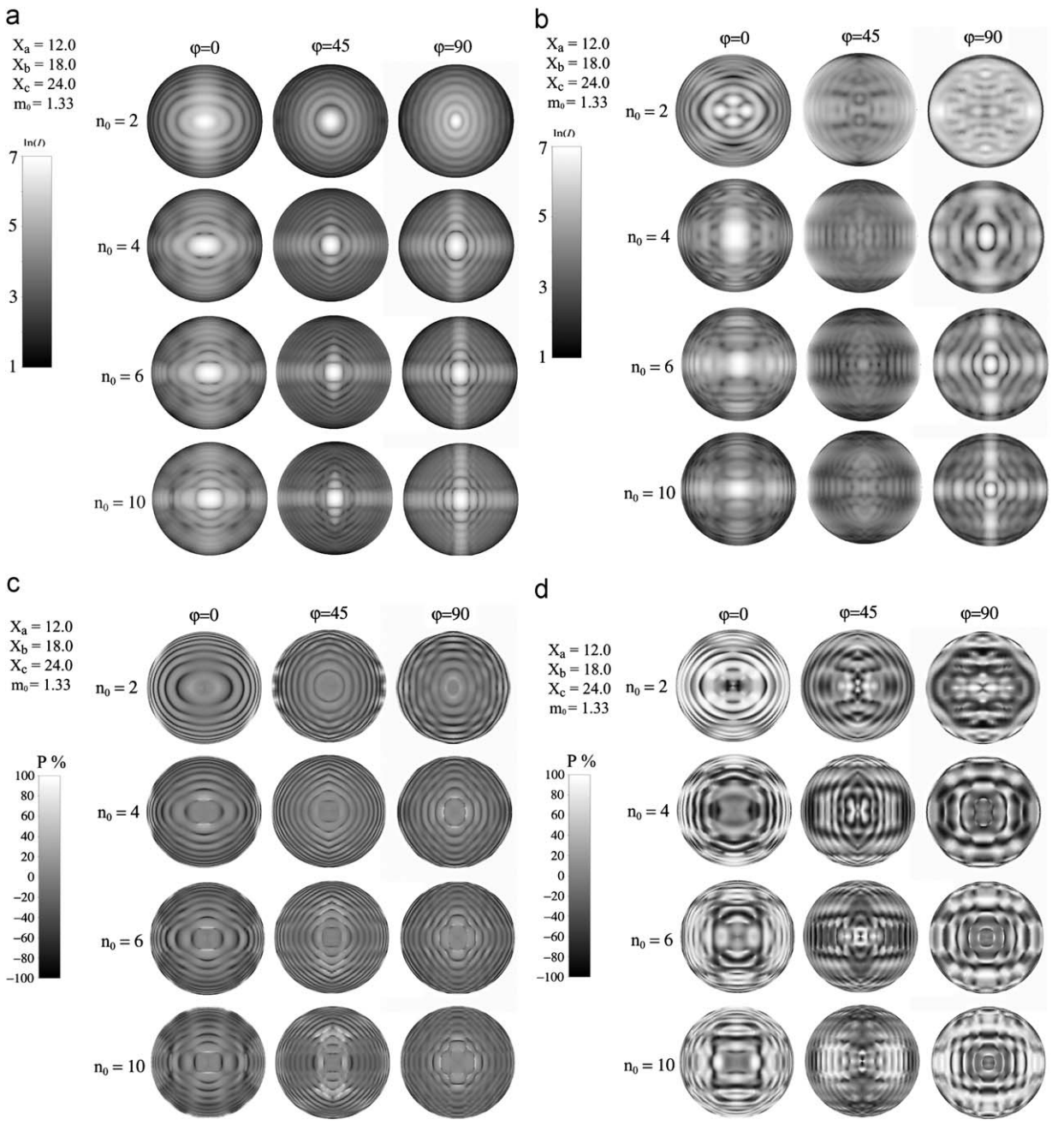

Fig. 2. Maps of the light-scattering intensity distributions of cuboid-like particles (m_0=1.33 and size parameters X_a=12, X_b=18, X_c=24) in the forward (a) and backward (b) hemispheres. The degree of linear polarization is presented in (c) (forward hemisphere) and (d) (backward hemisphere). The rows in these figures correspond to particle shapes changing from ellipsoid (n_0=2) at the top to more cuboid-like particles (n_0=10) at the bottom. The columns correspond to the fixed orientation of particles at different angles φ of electromagnetic wave incidence. At φ=0° the incident wave propagates parallel to the normal of the largest cuboid face. At φ=45° the incident wave propagates at an angle 45° to this normal, and at φ=90°, the incident wave propagates parallel to the normal to the smallest cuboid face.

influences the phase curves of intensity and, especially, the polarization degree. In particular, at small phase angles α ($\alpha=\pi-\vartheta$) the ellipsoid does not have negative polarization branch; whereas, one is present in all cuboid-like particles. Fig. 4 presents the normalized intensity and degree of linear polarization of cuboids averaged over orientation when one of the three dimensions is varied. Two size parameters are kept constant at $X_a=X_b=32$, while the third size parameter is varied from $X_c=2$ (plates) to $X_c=32$ (cube-like). The relatively large size parameters account for the high-frequency structure in the phase curves. While all particles demonstrate enhance in the

Please cite this article as: Petrov D, et al. Electromagnetic wave scattering from cuboid-like particles using *Sh*-matrices. JQSRT (2010), doi:10.1016/j.jqsrt.2010.01.024

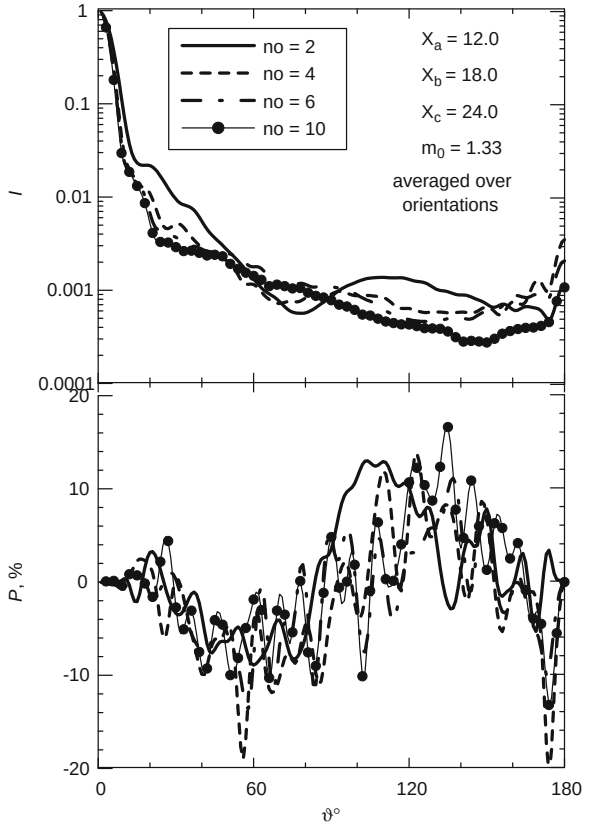

Fig. 3. The normalized intensity and degree of linear polarization of cuboid-like particles averaged over orientation. Curves are shown for particles having n_0=2 (solid lines), n_0=4 (dot lines), n_0=6 (dash-dot lines) and n_0=10 (lines with points), whose size parameters are X_a=12, X_b=18, X_c=24 and the refractive index is m_0=1.33.

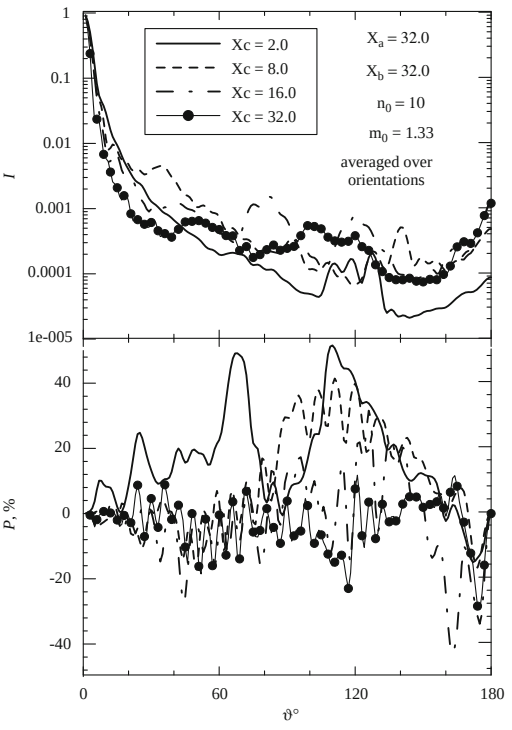

Fig. 4. The normalized intensity and degree of linear polarization of cuboids (square plates) averaged over orientation, whose basis is a square with X_a=X_b=32 and X_c that varies from 2 to 32; m_0=1.33 and n_0=10.

backscattering intensity and a significant negative polarization branch, a significant positive polarization branch is only present when the third size parameter is small. Fig. 5 shows the normalized intensity and degree of linear polarization for crystals of two minerals, olivine and topaz, which are averaged over orientations. For olivine, the ratio of the dimensions are a:b:c=0.466:1:0.589 and m_0=1.67; for mineral topaz a:b:c=0.528:1:0.954 and m_0=1.63. The size parameters of these crystals were chosen to be equal to those of the sphere of equal volume, having X=5.0. While the intensity phase functions do not vary significantly between the two types of particles, the polarization phase functions are significantly different. These calculations can be used as a benchmark in optical studies of the minerals.

To verify our theory and code, we have compared *Sh*-matrix calculations with those made using the discrete-dipole approximation (DDA) [14]. Fig. 6 shows the dependence of intensity and degree of linear polarization as a function of the scattering angle ϑ for cuboid-like particle with the following parameters: n_0=20, X_a=5.0, X_b=7.5, X_c=10.0 and m_0=1.5+0.1i. The particles are oriented so that the incident electromagnetic is perpendicular to the largest cuboid face. Points and solid lines correspond to the calculations carried out by

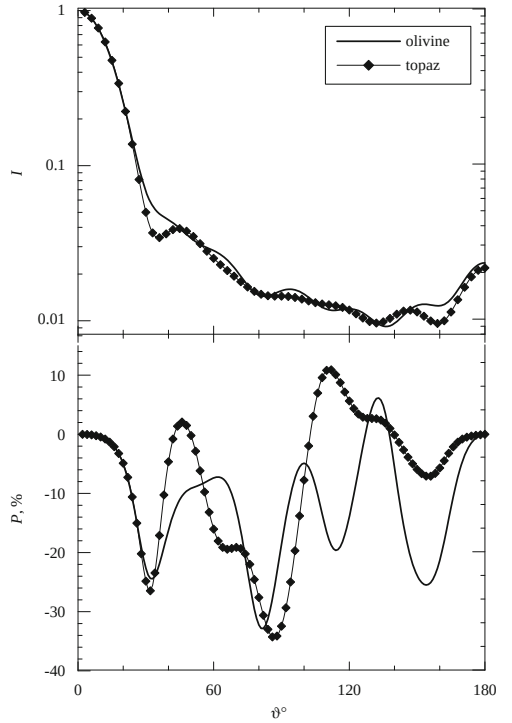

Fig. 5. The normalized intensity and degree of linear polarization of crystals of olivine and topaz, averaged over orientations. For olivine a:b:c=0.466:1:0.589 and m_0=1.67. For topaz a:b:c=0.528:1:0.954 and m_0=1.63. The volume of these crystals was chosen to be equal to X=5.0 spheres.

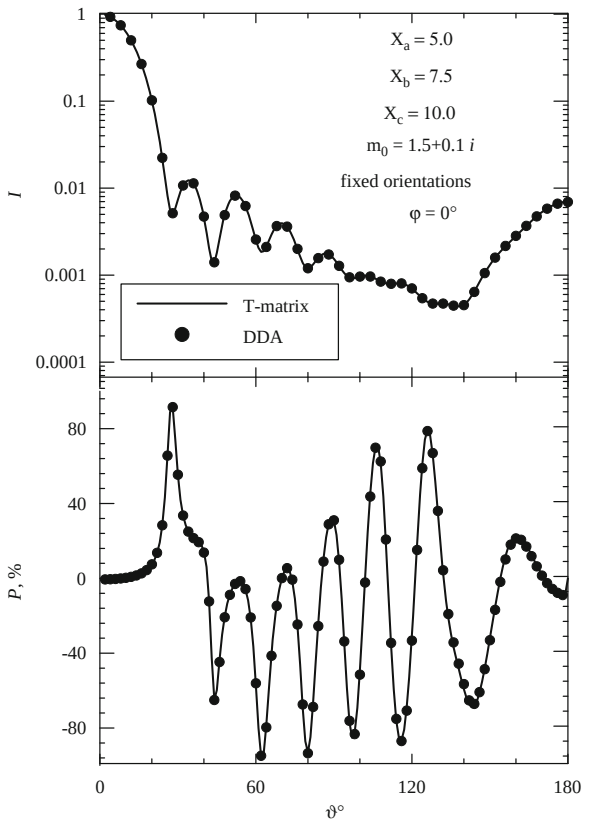

Fig. 6. The intensity and degree of linear polarization of a cuboid-like particle in a fixed orientation illuminated by an incident electromagnetic wave propagating perpendicular to the largest cuboid face. The following parameters are used: n_0=20, X_a=5.0, X_b=7.5, X_c=10.0 and m_0=1.5+0.1i. Points correspond to the calculations carried out with the DDA method in Zubko's version [14] and solid lines are calculations with the *Sh*-matrices method.

means of DDA and *Sh*-matrices methods, respectively. As can be seen, the curves coincide very well.

It also should be noted that the analytical solutions give significant acceleration of calculations as compared to the direct computation of the surface integrals dependently on the size parameter of particles; however, the primary time-consuming portion of the calculations remains computing the inverse matrix that is common for all variations of the *T*-matrix method.

4. Conclusion

We have used the *Sh*-matrix approach to derive analytical solutions for a family of shapes representing cuboid-like particles. Ellipsoids and pure cuboids are two extreme cases from this family. For cuboid-like particles edge diffraction bands are a dominant characteristic of the scattering patterns giving cross-like structure in the angular distributions of the intensity and degree of polarization. Although analytical solutions significantly accelerate calculations of scattering characteristic, the main time-consuming step remains computing the inverse matrix.

Acknowledgments

The authors thank E. Zubko for giving in their disposal his DDA code for the comparing calculations. This work was supported by the Army Medical Research Institute of Chemical Defense (Lucille Lumley, Ph.D.) under the auspices of the US Army Research Office Scientific Services Program administered by Battelle (Delivery Order 0378, Contract No. W911NF-07-D-0001).

Appendix A

In this appendix we present general expressions for the *Sh*-matrix elements of the *T*-matrix

$$\mathrm{Rg}Sh^{11}_{mnm'n',k} = -i\pi\frac{(-1)^{m'-m+k}}{2^{2k+n'+n+2}}A_{nn'}I^{(1)}_{mnm'n'}(2k+n+n'+2), \tag{A.1}$$

$$\mathrm{Rg}Sh^{121}_{mnm'n',k} = \pi\frac{(-1)^{m'-m+k}}{2^{2k+n'+n+2}}A_{nn'}\left[\begin{array}{l}(n+1)I^{(2)}_{mnm'n'}(2k+n+n'+1)\\ +L^{(01)}_{mnm'n'}(2k+n+n')+iL^{(10)}_{mnm'n'}(2k+n+n'+1)\end{array}\right], \tag{A.2}$$

$$\mathrm{Rg}Sh^{122}_{mnm'n',k} = -\pi\frac{(-1)^{m'-m+k}}{2^{2k+n'+n+3}}A_{nn'}I^{(2)}_{mnm'n'}(2k+n+n'+3), \tag{A.3}$$

$$\mathrm{Rg}Sh^{211}_{mnm'n',k} = -\pi\frac{(-1)^{m'-m+k}}{2^{2k+n'+n+2}}A_{nn'}\left[\begin{array}{l}(n'+1)I^{(2)}_{mnm'n'}(2k+n+n'+1)\\ L^{(01)}_{m'n'mn}(2k+n+n')-iL^{(10)}_{m'n'mn}(2k+n+n'+1)\end{array}\right], \tag{A.4}$$

$$\mathrm{Rg}Sh^{212}_{mnm'n',k} = \pi\frac{(-1)^{m'-m+k}}{2^{2k+n'+n+3}}A_{nn'}I^{(2)}_{mnm'n'}(2k+n+n'+3), \tag{A.5}$$

Please cite this article as: Petrov D, et al. Electromagnetic wave scattering from cuboid-like particles using *Sh*-matrices. JQSRT (2010), doi:10.1016/j.jqsrt.2010.01.024

$$\mathrm{Rg}Sh^{221}_{mnm'n',k} = -i\pi\frac{(-1)^{m'-m+k}}{2^{2k+n'+n+2}}A_{nn'}\left[\begin{array}{l}(n'+1)(n+1)I^{(0)}_{mnm'n'}(2k+n+n')\\ \quad+(n'+1)L^{(00)}_{mnm'n'}(2k+n+n'-1)+i(n'+1)L^{(11)}_{mnm'n'}(2k+n+n')\\ \quad+(n+1)L^{(00)}_{m'n'mn}(2k+n+n'-1)+i(n+1)L^{(11)}_{m'n'mn}(2k+n+n')\end{array}\right] \tag{A.6}$$

$$\mathrm{Rg}Sh^{222}_{mnm'n',k} = i\pi\frac{(-1)^{m'-m+k}}{2^{2k+n'+n+3}}A_{nn'}\left[\begin{array}{l}(n+1)I^{(0)}_{mnm'n'}(2k+n+n'+2)\\ +L^{(00)}_{mnm'n'}(2k+n+n'+1)-iL^{(11)}_{mnm'n'}(2k+n+n'+2)\end{array}\right] \tag{A.7}$$

$$\mathrm{Rg}Sh^{223}_{mnm'n',k} = i\pi\frac{(-1)^{m'-m+k}}{2^{2k+n'+n+3}}A_{nn'}\left[\begin{array}{l}(n'+1)I^{(1)}_{mnm'n'}(2k+n+n'+2)\\ +L^{(00)}_{m'n'mn}(2k+n+n'+1)-iL^{(11)}_{m'n'mn}(2k+n+n'+2)\end{array}\right], \tag{A.8}$$

$$\mathrm{Rg}Sh^{224}_{mnm'n',k} = -i\pi\frac{(-1)^{m'-m+k}}{2^{2k+n'+n+4}}A_{nn'}I^{(1)}_{mnm'n'}(2k+n+n'+4), \tag{A.9}$$

$$Sh^{11}_{mnm'n',k} = \pi\frac{(-1)^{m'-m+n-1+k}}{2^{2k+n'-n+1}}A_{nn'}I^{(1)}_{mnm'n'}(2k-n+n'+1), \tag{A.10}$$

$$Sh^{121}_{mnm'n',k} = i\pi\frac{(-1)^{m'-m+n-1+k}}{2^{2k+n'-n+1}}A_{nn'}\left[\begin{array}{l}-nI^{(2)}_{mnm'n'}(2k-n+n')\\ +L^{(01)}_{mnm'n'}(2k-n+n'-1)+L^{(10)}_{mnm'n'}(2k-n+n')\end{array}\right] \tag{A.11}$$

$$Sh^{122}_{mnm'n',k} = -i\pi\frac{(-1)^{m'-m-n+1+k}}{2^{2k+n'-n+2}}A_{nn'}I^{(2)}_{mnm'n'}(2k-n+n'+2), \tag{A.12}$$

$$Sh^{211}_{mnm'n',k} = -i\pi\frac{(-1)^{m'-m-n-1+k}}{2^{2k+n-n+1}}A_{nn'}\left[\begin{array}{l}(n'+1)I^{(2)}_{mnm'n'}(2k-n+n')\\ +L^{(00)}_{mnm'n'}(2k-n+n'-1)-iL^{(11)}_{mnm'n'}(2k-n+n')\end{array}\right] \tag{A.13}$$

$$Sh^{212}_{mnm'n',k} = i\pi\frac{(-1)^{m'-m-n-1+k}}{2^{2k+n'-n+1}}A_{nn'}I^{(2)}_{mnm'n'}(2k-n+n'+2), \tag{A.14}$$

$$Sh^{221}_{mnm'n',k} = \pi\frac{(-1)^{m'-m-n-1+k}}{2^{2k+n'-n+1}}A_{nn'}\left[\begin{array}{l}-n(n'+1)I^{(1)}_{mnm'n'}(2k-n+n'-1)\\ +(n'+1)L^{(00)}_{mnm'n'}(2k-n+n'-2)+i(n'+1)L^{(11)}_{mnm'n'}(2k-n+n'-1)\\ -nL^{(00)}_{m'n'mn}(2k-n+n'-2)+inL^{(11)}_{m'n'mn}(2k-n+n'-1)\end{array}\right] \tag{A.15}$$

$$Sh^{222}_{mnm'n',k} = -\pi\frac{(-1)^{m'-m-n-1+k}}{2^{2k+n'-n+2}}A_{nn'}\left[\begin{array}{l}-nI^{(1)}_{mnm'n'}(2k-n+n'+1)\\ +L^{(00)}_{mnm'n'}(2k-n+n')+iL^{(11)}_{mnm'n'}(2k-n+n'+1)\end{array}\right], \tag{A.16}$$

$$Sh^{223}_{mnm'n',k} = \pi\frac{(-1)^{m'-m-n-1+k}}{2^{2k+n'-n+2}}A_{nn'}\left[\begin{array}{l}(n'+1)I^{(1)}_{mnm'n'}(2k-n+n'+1)\\ +L^{(00)}_{m'n'mn}(2k-n+n')-iL^{(11)}_{m'n'mn}(2k-n+n'+1)\end{array}\right] \tag{A.17}$$

$$Sh^{224}_{mnm'n',k} = \pi\frac{(-1)^{m'-m-n+1+k}}{2^{2k+n'-n+3}}A_{nn'}I^{(1)}_{mnm'n'}(2k-n+n'+3). \tag{A.18}$$

The following designations are used in formulae (A.1)–(A.18)

$$I^{(1)}_{mnm'n'}(z) = m\left[\frac{n'\sqrt{(n'+1)^2-m'^2}}{2n'+1}I^{(\theta)}_{mnm'n'+1}(z)-\frac{(n'+1)\sqrt{n'^2-m'^2}}{2n'+1}I^{(\theta)}_{mnm'n'-1}(z)\right]$$
$$+m'\left[\frac{n\sqrt{(n+1)^2-m^2}}{2n+1}I^{(\theta)}_{mn+1m'n'}(z)-\frac{(n+1)\sqrt{n^2-m^2}}{2n+1}I^{(\theta)}_{mn-1m'n'}(z)\right], \tag{A.19}$$

$$I^{(2)}_{mnm'n'}(z) = |mm'|I^{(\theta)}_{mnm'n'}(z)+\frac{1}{(2n'+1)(2n+1)}\left[(n'+1)\sqrt{n'^2-m'^2}(n+1)\sqrt{n^2-m^2}I^{(\theta)}_{mn-1m'n'-1}(z)\right.$$
$$\left.+n'\sqrt{(n'+1)^2-m'^2}n\sqrt{(n+1)^2-m^2}I^{(\theta)}_{mn+1m'n'+1}(z)-(n'+1)\sqrt{n'^2-m'^2}n\sqrt{(n+1)^2-m^2}I^{(\theta)}_{mn+1m'n'-1}(z)\right.$$

Please cite this article as: Petrov D, et al. Electromagnetic wave scattering from cuboid-like particles using *Sh*-matrices. JQSRT (2010), doi:10.1016/j.jqsrt.2010.01.024

$$-n'\sqrt{(n'+1)^2-m'^2}(n+1)\sqrt{n^2-m^2}I^{(\theta)}_{mn-1m'n'+1}(z)\Big], \tag{A.20}$$

where

$$L^{(00)}_{mnm'n'}(z)=m'I'^{(\theta)}_{mnm'n'}(z), \tag{A.21}$$

$$L^{(01)}_{mnm'n'}(z)=\frac{1}{2n'+1}\left[n'\sqrt{(n'+1)^2-m'^2}I'^{(\theta)}_{mnm'n'+1}(z)-(n'+1)\sqrt{n'^2-m'^2}I'^{(\theta)}_{mnm'n'-1}(z)\right], \tag{A.22}$$

$$L^{(10)}_{mnm'n'}(z)=m'I^{(\varphi)}_{mnm'n'}(z), \tag{A.23}$$

$$L^{(11)}_{mnm'n'}(z)=\frac{1}{2n'+1}\left[n'\sqrt{(n'+1)^2-m'^2}I^{(\varphi)}_{mnm'n'+1}(z)-(n'+1)\sqrt{n'^2-m'^2}I^{(\varphi)}_{mnm'n'-1}(z)\right], \tag{A.24}$$

and

$$\begin{aligned}I^{(\theta)}_{mnm'n'}(z)=&(-1)^{n+n'}\Xi_m\Xi_{m'}n!\sqrt{(n-|m|)!(n+|m|)!}n'!\sqrt{(n'-|m'|)!(n'+|m'|)!}\sum_{k=0}^{n-|m|}\frac{(-1)^k}{k!(n-k)!(n-|m|-k)!(|m|+k)!}\\&\times\sum_{k'=0}^{n'-|m'|}\frac{(-1)^{k'}}{k'!(n'-k')!(n'-|m'|-k')!(|m'|+k')!}[I^{(C1)}(m'-m,2n-2k-|m|+2n'-2k'-|m'|-1,2k\\&+|m|+2k'+|m'|-1,z)],\end{aligned} \tag{A.25}$$

$$\begin{aligned}I'^{(\theta)}_{mnm'n'}(z)=&(-1)^{n+n'}\Xi_m\Xi_{m'}n!\sqrt{(n-|m|)!(n+|m|)!}n'!\sqrt{(n'-|m'|)!(n'+|m'|)!}\sum_{k=0}^{n-|m|}\frac{(-1)^k}{k!(n-k)!(n-|m|-k)!(|m|+k)!}\\&\times\sum_{k'=0}^{n'-|m'|}\frac{(-1)^{k'}}{k'!(n'-k')!(n'-|m'|-k)!(|m'|+k')!}[I^{(C2)}(m'-m,2n-2k-|m|+2n'-2k'-|m'|,2k+|m|+2k'+|m'|,z)]\end{aligned} \tag{A.26}$$

$$\begin{aligned}I^{(\varphi)}_{mnm'n'}(z)=&(-1)^{n+n'}\Xi_m\Xi_{m'}n!\sqrt{(n-|m|)!(n+|m|)!}n'!\sqrt{(n'-|m'|)!(n'+|m'|)!}\sum_{k=0}^{n-|m|}\frac{(-1)^k}{k!(n-k)!(n-|m|-k)!(|m|+k)!}\\&\times\sum_{k'=0}^{n'-|m'|}\frac{(-1)^{k'}}{k'!(n'-k')!(n'-|m'|-k')!(|m'|+k')!}[I^{(C3)}(m'-m,2n-2k-|m|+2n'-2k'-|m'|,2k+|m|+2k'+|m'|,z)],\end{aligned} \tag{A.27}$$

where

$$\begin{aligned}I^{(C1)}(m,\eta,v,z)=&\sum_{p=0}^{\infty}\frac{\frac{z}{n_0}\left(\frac{z}{n_0}-1\right)\dots\left(\frac{z}{n_0}-p+1\right)}{p!}\sum_{p'=0}^{p}(-1)^{p'}C_p^{p'}\Phi(m,p')\\&\times\sum_{k=0}^{p-p'}\frac{C_{p-p'}^{k}}{c^{n_0k}}\sum_{k'=0}^{n_0k}(-2)^{k'}C_{n_0k}^{k'}\Omega(v+n_0p'+2k',\eta+n_0p'),\end{aligned} \tag{A.28}$$

$$\begin{aligned}I^{(C2)}(m,\eta,v,z)=&2\sum_{p=0}^{\infty}\frac{\left(\frac{z+1}{n_0}+1\right)\left(\frac{z+1}{n_0}\right)\dots\left(\frac{z+1}{n_0}-p+2\right)}{p!}\sum_{p'=0}^{p}(-1)^{p'}C_p^{p'}\Phi(m,p')\\&\times\sum_{k=0}^{p-p'}\frac{C_{p-p'}^{k}}{c^{n_0k+n_0}}\sum_{k'=0}^{n_0k+n_0-1}(-2)^{k'}C_{n_0k}^{k'}\Omega(v+n_0p'+2k'+1,\eta+n_0p'+1)-2^{n_0-1}\\&\times\sum_{p=0}^{\infty}\frac{\left((z+1/n_0)+1\right)(z+1/n_0)\dots\left((z+1/n_0)-p+2\right)}{p!}\sum_{p'=0}^{p}(-1)^{p'}C_p^{p'}\Phi(m,p'+1)\\&\times\sum_{k=0}^{p-p'}\frac{C_{p-p'}^{k}}{c^{n_0k+1}}\sum_{k'=0}^{n_0k+1}(-2)^{k'}C_{n_0k}^{k'}\Omega(v+n_0p'+2k'+n_0-1,\eta+n_0p'+n_0-1),\end{aligned} \tag{A.29}$$

$$\begin{aligned}I^{(C3)}(m,\eta,v,z)=&-2^{n_0}\sum_{p=0}^{\infty}\frac{\left(\frac{z+1}{n_0}+1\right)\left(\frac{z+1}{n_0}\right)\dots\left(\frac{z+1}{n_0}-p+2\right)}{p!}\sum_{p'=0}^{p}(-1)^{p'}C_p^{p'}\Theta(m,p')\\&\times\sum_{k=0}^{p-p'}\frac{C_{p-p'}^{k}}{c^{n_0k+n_0-1}}\sum_{k'=0}^{n_0k+n_0-1}(-2)^{k'}C_{n_0k}^{k'}\Omega(v+n_0p'+2k'+n_0,\eta+n_0p'+n_0)\end{aligned} \tag{A.30}$$

where

$$\Phi(m,p)=\sum_{k=0}^{p}C_p^k\frac{i\pi\exp[i\pi(m-n_0p+n_0k-1/2)]\left(1+\exp[i\pi m](-1)^{n_0p}\right)}{a^{n_0k}b^{n_0p-n_0k}2^{n_0p}(n_0k+1)\mathrm{B}\left(\frac{n_0p-m}{2}+1,\frac{n_0p-m}{2}+2\right)}\,{}_2F_1\left(n_0k-n_0p,\frac{m-n_0p}{2};1+\frac{2n_0k-n_0p+m}{2};-1\right) \tag{A.31}$$

Please cite this article as: Petrov D, et al. Electromagnetic wave scattering from cuboid-like particles using *Sh*-matrices. JQSRT (2010), doi:10.1016/j.jqsrt.2010.01.024

$$\Omega(\eta,\nu)=\frac{\Gamma\left(\frac{\eta+1}{2}\right)\Gamma\left(\frac{\nu+1}{2}\right)}{2\Gamma\left(\frac{\eta+\nu}{2}+1\right)} \tag{A.32}$$

$$\begin{aligned}\Theta(m,p)=&\sum_{k=0}^{p}C_p^k\frac{i\pi\exp[i\pi(m-n_0p+n_0k-2/2)]\left(1+\exp[i\pi m](-1)^{n_0p}\right)}{a^{n_0k+n_0-1}b^{n_0p-n_0k+1}2^{n_0p+n_0}(n_0k+n_0)\mathrm{B}\left((n_0p+n_0-m/2)+1,(2n_0k-n_0p+n_0+m/2)\right)}\\&\times{}_2F_1\left(n_0k-n_0p-1,(m-n_0p-\nu/2);(2n_0k-n_0p+n_0+m/2);-1\right)\\&-\sum_{k=0}^{p}C_p^k\frac{i\pi\exp[i\pi(m-n_0p+n_0k-n_0/2)]\left(1+\exp[i\pi m](-1)^{n_0p}\right)}{a^{n_0k+1}b^{n_0p-n_0k+n_0-1}2^{n_0p+n_0}(n_0k+2)\mathrm{B}\left((n_0p+n_0-m/2)+1,(2n_0k-n_0p-n_0-m/2)+2\right)}\\&\times{}_2F_1\left(n_0k-n_0p-n_0+1,(m-n_0p-n_0/2);(2n_0k-n_0p-n_0-m/2)+2;-1\right)\end{aligned} \tag{A.33}$$

where ${}_2F_1$ is the Gaussian hypergeometrical function

$${}_2F_1(a_1,a_2;b_1;z)=\frac{\Gamma(b_1)}{\Gamma(a_1)\Gamma(a_2)}\sum_{n=0}^{\infty}\frac{\Gamma(a_1+n)\Gamma(a_2+n)}{\Gamma(b_1+n)}\frac{z^n}{n!}, \tag{A.34}$$

$B(n,m)$ is the Beta-function

$$B(n,m)=\frac{\Gamma(n)\Gamma(m)}{\Gamma(n+m)}, \tag{A.35}$$

$$\Xi_m=\begin{cases}1, & m\geq 0\\(-1)^m, & m<0,\end{cases} \tag{A.36}$$

$$A_{nn'}=\sqrt{\frac{(2n'+1)}{4\pi n'(n'+1)}}\sqrt{\frac{(2n+1)}{4\pi n(n+1)}} \tag{A.37}$$

and $C_n^m=(n!/m!(n-m)!)$ are the binomial coefficients.

References

[1] Hurlbut CS, Klein C. Manual of mineralogy. New York: John Wiley and Sons; 1985 596 pp..
[2] Tsang L, Kong J, Shin R. Theory of microwave remote sensing. New York: John Wiley and Sons; 1985 603 pp..
[3] Mishchenko MI, Travis LD, Mackowski DW. T-matrix computations of light scattering by nonspherical particles: a review. JQSRT 1996;55:535–73.
[4] Petrov D, Synelnyk E, Shkuratov Y, Videen G. The T-matrix technique for calculations of scattering properties of ensembles of randomly oriented particles with different size. JQSRT 2006;102:85–110.
[5] Mishchenko MI, Travis LD, Lacis AA. Scattering, absorption, and emission of light by small particles. Cambridge: Cambridge University Press; 2002 445 pp..
[6] Petrov D, Shkuratov Yu, Videen G. The *Sh*-matrices method as applied to scattering by microlenses. JQSRT 2009;110:1448–59.
[7] Petrov D, Shkuratov Y, Videen G. Analytical light-scattering solution for Chebyshev particles. JOSA A 2007;24(4):1103–19.
[8] Petrov D, Videen G, Shkuratov Y, Kaydash M. Analytic T-matrix solution of light scattering from capsule and bi-sphere particles: applications to spore detection. JQSRT 2007;108:81–105.
[9] Petrov D, Shkuratov Y, Videen G. Analytic light-scattering solution of two merging spheres using Sh-matrices. Opt Commun 2008;281: 2411–23.
[10] Petrov D, Shkuratov Y, Videen G. Sh-matrices method applied to light scattering by finite circular cylinders. JQSRT 2008;109:1474–95.
[11] Petrov D, Shkuratov Y, Videen G. Influence of corrugation on light-scattering properties of capsule and finite-cylinder particles: analytic solution using Sh-matrices. JQSRT 2008;109:650–69.
[12] Petrov D, Shkuratov Y, Videen G. An analytical solution to the light scattering from cube-like particles using Sh-matrices. JQSRT 2010.
[13] Petrov D, Shkuratov Y, Videen G. Sh-matrices method as applied to scattering by particles with layered structure. JQSRT 2007;106: 43775.
[14] Penttila A, Zubko E, Lumme K, Muinonen K, Yurkin M, Draine B, et al. Comparison between discrete dipole implementations and exact techniques. JQSRT 2007;106:417–36.

Please cite this article as: Petrov D, et al. Electromagnetic wave scattering from cuboid-like particles using *Sh*-matrices. JQSRT (2010), doi:10.1016/j.jqsrt.2010.01.024